sustainability

MDPI

Article

R4-Graph: Integrating Sustainability into Discrete Mathematics Education Through Resilience-Oriented Graph Theory

Ru Zhang [1], Lihong Li [1], Chundong Liang [1,2] and Yafeng Yang [1,3,*]

[1] College of Sciences, North China University of Science and Technology, Tangshan 063210, China; zhangru@ncst.edu.cn (R.Z.); kysl@ncst.edu.cn (L.L.); liangchundong@ncst.edu.cn (C.L.)
[2] School of Computer Science and Technology, Tianjin University, Tianjin 300350, China
[3] State Key Laboratory of Hydraulic Engineering Intelligent Construction and Operation, Tianjin University, Tianjin 300350, China
* Correspondence: hblgyyf@ncst.edu.cn

Abstract

The Education for Sustainable Development approach calls for mathematical tasks that illuminate the structure and changing behaviour of interdependent systems. This study develops R4-Graph, a four-phase sequence for sustainability-oriented discrete mathematics: Represent, Remove, Recover, and Redesign. The framework connects system modelling, vulnerability analysis, restoration strategies, and constrained network design through common graph representations and explicit mathematical tasks. Computational experiments covered 360 synthetic disturbance networks, 40 recovery networks, and 2112 link addition configurations across 12 spatial graphs; archived trajectories from the Catlins stream food web provided an environmental illustration. In preferential attachment networks, mean resilience was 0.5601 under random removal and 0.3776 under degree-targeted removal. Betweenness priority restoration yielded recovery resilience of 0.6817, compared with 0.6307 under random restoration. Spatial redesign exposed resilience–cost trade-offs, diminishing marginal improvements, and sensitivity to candidate edge selection. These results inform a four-stage teaching sequence with specified mathematical objectives, computational artefacts, and decision-making tasks for undergraduate discrete mathematics.

Keywords: education for sustainable development; discrete mathematics; graph theory; network resilience; task design; computational reconstruction; systems thinking; mathematical modelling; multi-objective decision-making

Check for updates

Academic Editors: Maite M. Aldaya, María Napal and María J. Cantalejo

Received: 10 October 2026
Revised: 23 October 2026
Accepted: 2 November 2026
Published: 4 November 2026

Copyright: © 2026 by the authors. Licensee MDPI, Basel, Switzerland. This article is an open access article distributed under the terms and conditions of the Creative Commons Attribution (CC BY) license.

1. Introduction

Discrete mathematics has a distinctive educational role because it makes structures, relations, finite change, algorithms, and decision processes explicit. Networks, combinatorial reasoning, algorithmic problem solving, discrete modelling, and optimisation are central to the field [1]. Graph-based modelling represents relational systems as mathematical objects and links representation to optimisation [2,3]. These features make graph theory well suited to systems-oriented curriculum design.

Education for Sustainable Development (ESD) reinforces this systems orientation. UNESCO identifies systems thinking, anticipatory thinking, critical thinking, collaboration, and integrated problem solving as competencies for sustainable development [4], while the ESD 2030 roadmap calls for curricula oriented toward achieving the SDGs [5]. Research on sustainability competencies likewise emphasises systems thinking in addressing interdependent socio-ecological problems [6,7], and future-oriented higher education frameworks

highlight systemic, anticipatory, and critical reasoning [8]. Meaningful curricular integration requires disciplinary knowledge, problem orientation, multiple perspectives, and pedagogical structures that connect sustainability competencies with the organisation of learning [9,10].

Recent studies have connected mathematics and sustainability through mathematical modelling [11], statistics education [12], and systems thinking and simulation [13]. Reviews identify curriculum, pedagogy, modelling, and mathematical task design as priorities for further development [14,15]. A systematic review has also called for stronger empirical investigation of education for sustainable development in mathematics [16]. Research on mathematics education and uncertainty highlights the value of reasoning about changing and interdependent systems [17]. These perspectives inform the design of graph-theoretic tasks that connect modelling choices, system vulnerability, restoration, and adaptation.

Network-based approaches have used graphs to examine interrelations among the Sustainable Development Goals [18]. Building on this relational perspective, R4-Graph considers how a network responds to disruption, how its connectivity can be restored, and which adaptations are feasible under resource constraints. These questions form a connected sequence of graph-theoretic tasks centred on the changing state of a system.

Resilience provides the conceptual bridge. In ecology, resilience emphasises persistence and the capacity to absorb change [19]; engineering and community-resilience frameworks add dimensions such as robustness, redundancy, resourcefulness, and rapidity [20]. Reviews emphasise that resilience is multidimensional rather than reducible to one universal metric [21], while quantitative frameworks distinguish absorptive, restorative, and adaptive capacities [22] and broader resilience scholarship emphasises response and adaptation under uncertain disruption [23]. Network-based infrastructure research similarly treats resilience as system behaviour under disruption [24], and resilience curve approaches make performance loss and recovery over time explicit [25].

Graph theory provides established representations and analytical tools for describing network structure, connectivity, and dynamics [26,27]. In graph-theoretic terms, robustness considers what remains after failures; recovery considers how functionality returns and whether restoration order matters; adaptation considers whether to redesign rather than restore. These distinctions motivate the R4-Graph framework: Represent–Remove–Recover–Redesign, organising graph-theoretic reasoning around modelling, disturbance, restoration, and constrained redesign.

This study develops R4-Graph as a connected sequence of sustainability-oriented graph theory tasks and establishes a computational basis for its design. The framework integrates four forms of mathematical reasoning within a shared network model: specifying representations, analyzing structural vulnerability, comparing restoration sequences, and evaluating feasible adaptations under resource constraints. The experiments provide quantitative cases for task selection, while the accompanying curricular specification identifies learning objectives, student artefacts, and opportunities for mathematical explanation and justification.

2. Materials and Methods

2.1. Research Design and Framework Development

The research combined conceptual curriculum design and quantitative network analysis. We mapped resilience-related decisions to graph-theoretic concepts, operations, and student-produced mathematical artefacts, then examined these relationships using controlled graph ensembles. Independent graph instances and their disturbance, restoration, and redesign outcomes were the computational units of analysis.

The conceptual mapping was developed by the authors from discrete mathematics concepts, the resilience literature [19,22,23], and research on mathematics task design. Four guiding questions structured the mapping: How should a relational system be represented? How does it respond to specified disruptions? Which restoration order improves intermediate performance? Which feasible structural adaptation offers an acceptable resilience–cost trade-off? Each question was linked to graph operations, measurable outputs, and potential student explanations.

R4-Graph was developed through a conceptual mapping procedure that integrated established forms of reasoning in discrete mathematics—modelling, structural reasoning, algorithmic reasoning, and optimisation—with resilience processes identified in ecological and engineered-systems research.

This framework development was guided by five design criteria:

1. Disciplinary fidelity: Each phase had to correspond to established graph-theoretic objects, operations, or problems rather than function as a metaphorical label alone.
2. Resilience correspondence: The phases had to represent distinct processes of system representation, disturbance and resistance, recovery, and adaptive redesign.
3. Curricular continuity: The sequence had to connect modelling, structural reasoning, algorithmic ordering, and optimisation within one evolving graph.
4. Computability: Each phase had to yield mathematical quantities, trajectories, or decisions that could be formally defined and reproduced.
5. Context portability: The same mathematical architecture had to remain interpretable across different sustainability-related network contexts.

Together, these criteria shaped a sequence in which a graph model can be revisited under changing conditions and decisions. The computational experiments then characterised the distinct outputs associated with disturbance, recovery, and redesign, providing a basis for selecting and sequencing graph-theoretic tasks. Context portability refers to the use of the four-stage task structure with different relational systems. In each application, learners specify the node and edge meanings, select a relevant disturbance scenario, and interpret performance measures in the context of the model.

2.2. The R4-Graph Framework

Figure 1 illustrates how resilience and sustainability organise graph theory content across the four phases of Represent, Remove, Recover, and Redesign.

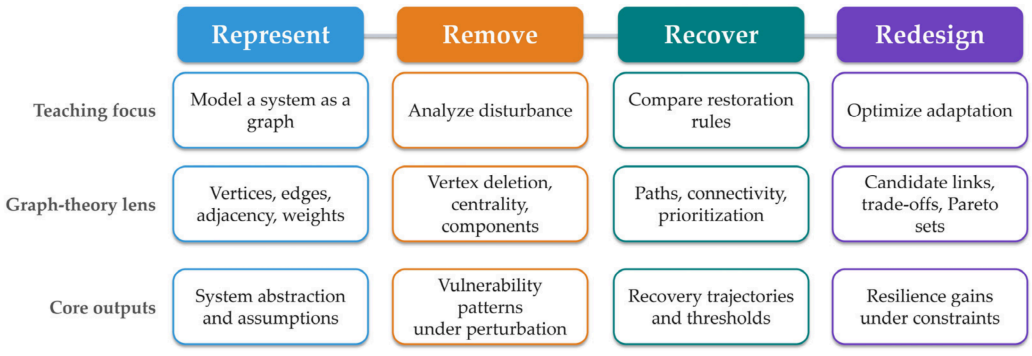


Figure 1. The four phases of the R4-Graph framework.

The four phases are linked by a common network representation but differ in the question posed. Represent establishes modelling assumptions; Remove examines vulnerability under specified disturbances; Recover compares trajectories generated by alternative restoration rules; and Redesign evaluates feasible interventions under resource constraints.

This progression connects foundational graph concepts to systems-level reasoning about resilience and resource allocation.

2.2.1. Represent

A sustainability-related system δ is represented as

$$\delta \rightarrow G = (V, E, W) \tag{1}$$

where V represents system entities, E represents relations among them, and W, when applicable, represents edge weights. Weighted-network analysis illustrates how relational strength or cost can be treated as a mathematical property rather than merely a contextual annotation [28]. The intended curricular emphasis is on modelling assumptions: defining vertices, determining what constitutes an edge, selecting directionality and weights, and recognising what the graph deliberately omits.

2.2.2. Remove

Disturbance is represented through component deletion:

$$G_q = G - \Phi_q,\ q = \frac{|\Phi_q|}{|V_0|} \tag{2}$$

Random failures and targeted attacks can have different effects on heterogeneous networks [29–31], while network restructuring may reduce targeted vulnerability [32]. The Remove phase turns these mechanisms into alternative deletion rules. Comparing their consequences for connectivity and efficiency requires reasoning about how topology and the disturbance mechanism interact.

2.2.3. Recover

Recovery is represented as an ordered graph sequence:

$$G_0^-,\ G_1,\ \ldots,\ G_T \tag{3}$$

Different restoration strategies can reach the same final topology while generating different levels of intermediate performance. Recovery trajectories therefore provide mathematical objects for comparing algorithms and ordering decisions. Students can examine which vertices to restore first, how network performance changes at each step, and why final connectivity alone does not capture the recovery process.

2.2.4. Redesign

Redesign allows candidate edges that were not part of the original graph.

Binary variables

$$x_e \in \{0,1\} \tag{4}$$

indicate whether candidate edge e is added.

A generic budget-constrained problem can be written as:

$$\max_x R(G + x) \text{ subject to } \sum_{e \in E_c} c_e x_e \leq B \tag{5}$$

Equation (5) presents a general resilience maximisation problem with a resource budget. The computational Redesign experiment implements a cardinality constraint of at most three new links from a screened ten-edge candidate set and treats normalised spatial connection cost as a second objective. All feasible link addition combinations are exhaustively enumerated, and Pareto-nondominated designs are identified by evaluating degree-targeted disturbance resilience and spatial connection cost [33].

2.3. Computational Evaluation Design

2.3.1. Network Performance Measures

The three computational experiments correspond to the decision-focused R4-Graph phases. Remove measures performance loss under specified node removal rules; Recover compares restoration sequences using trajectory area and threshold indices; Redesign evaluates feasible link additions by disturbance resilience and spatial connection cost. Fixed-reference global efficiency is the principal performance measure, complemented by the relative largest connected component.

The primary performance measure was fixed-reference global efficiency. Standard global efficiency is based on reciprocal shortest path distance [34]. In a vertex deletion experiment, however, normalising only by surviving vertices can make a damaged graph appear artificially efficient after peripheral vertices are removed. The denominator was therefore fixed at the original system size n_0:

$$E^{(0)}(G_t) = \frac{1}{n_0(n_0-1)} \sum_{\substack{i \neq j \\ i,j \in V(G_t)}} \frac{1}{d_{ij}(t)} \tag{6}$$

For disconnected vertex pairs, the reciprocal distance contribution was defined as zero. Normalised performance is

$$P(t) = \frac{E^{(0)}(G_t)}{E^{(0)}(G_0)} \tag{7}$$

The relative largest connected component is

$$S(t) = \frac{|C_{\max}(G_t)|}{n_0} \tag{8}$$

Degree and betweenness centrality were used to define targeted removals and restoration priorities. Betweenness centrality measures the extent to which a vertex lies on shortest paths [35,36].

2.3.2. Synthetic Network Ensemble

Four graph families were selected to provide controlled contrasts in randomness, clustering, degree heterogeneity, and spatial embedding. Erdős–Rényi (ER) graphs provided a classical random graph baseline [37], Watts–Strogatz (WS) graphs represented clustered small-world structure [38], and Barabási–Albert (BA) graphs represented heterogeneous preferential attachment structure [39]. A spatial fixed-edge (SFE) condition introduced spatial embedding while maintaining a prescribed edge count [40].

For the disturbance experiment, $n \in \{50, 100, 200\}$ with a target mean degree of approximately ten. Thirty connected graphs were generated independently for each topology-by-size cell, yielding 360 graphs. ER graphs had exactly $5n$ edges; WS graphs used $k = 10$ and rewiring probability 0.15; BA graphs used attachment parameter $m = 5$. For spatial fixed-edge (SFE) graphs, n points were drawn uniformly in the unit square and the $5n$ shortest Euclidean vertex pairs were connected. Disconnected graph draws were rejected. Fractional deletion counts were obtained by rounding qn to the nearest integer, with halves rounded upwards. Random seeds and accepted graph instances were saved.

2.3.3. Disturbance Experiment

Each graph was subjected to random, degree-targeted, and betweenness-targeted vertex removal on the grid $q \in \{0, 0.05, 0.10, \ldots, 0.50\}$. One seeded random order was generated per graph; centrality-based orders used the baseline network. Resilience indices were computed from the full trajectories for each of the three conditions.

Degree- and betweenness-based target rankings were computed from the undisturbed graph and held fixed throughout each removal trajectory, thereby separating structural degradation from adaptive re-ranking.

The efficiency-based disturbance resilience index was

$$R_D^{(E)} = \frac{1}{q_{\max}} \int_0^{q_{\max}} P_E(q)\mathrm{d}q,\ q_{\max} = 0.50. \tag{9}$$

approximated using the trapezoidal rule. A component-based analogue was

$$R_D^{(S)} = \frac{1}{q_{\max}} \int_0^{q_{\max}} S(q)\mathrm{d}q. \tag{10}$$

The experiment produced 1080 graph-by-disturbance resilience indices and 11,880 performance observations. Graph instances, removal orders, and trajectory outputs were retained for reproducibility.

2.3.4. Recovery Experiment

The recovery experiment used 40 independently generated connected networks with $n = 100$ (ten per topology).

For each network, the 30 vertices with the highest baseline degree were removed. Four restoration strategies were evaluated from the same damaged state:

1. Random restoration: the mean trajectory across 50 independent seeded random restoration orders for each damaged graph.
2. Degree priority restoration: vertices restored in descending order of baseline degree.
3. Betweenness priority restoration: vertices restored in descending order of baseline betweenness centrality.
4. Static initial efficiency gain priority: vertices restored in descending order of their one-step marginal efficiency gain computed from the initial damaged state.

For the fourth rule,

$$g(v) = P(H_0 + v) - P(H_0) \tag{11}$$

Let H_0 be the damaged graph and $H_0 + v$ the state after restoring vertex v and its original incident edges.

For each structure-informed strategy, the baseline or initial-damaged-state ranking was computed once and then applied throughout the restoration sequence.

Normalised recovery progress was defined with t as the number of restored vertices and T as the total number of removed vertices:

$$\tau = \frac{t}{T},\ 0 \le \tau \le 1 \tag{12}$$

and recovery resilience was

$$R_R = \int_0^1 P_R(\tau)\mathrm{d}\tau \tag{13}$$

Threshold measures were

$$T_{80} = \min\{\tau{:}P_R(t) \ge 0.80\},\ T_{90} = \min\{\tau{:}P_R(t) \ge 0.90\} \tag{14}$$

T_{80} and T_{90} were defined as the earliest observed restoration fractions at which fixed-reference performance reached 0.80 and 0.90, respectively. Both thresholds were read from the 31-state discrete recovery trajectory.

2.3.5. Constrained Spatial Redesign

The spatial Redesign experiment used 12 independently generated connected SFE graphs, each with $n = 50$ vertices uniformly located in the unit square and $m = 250$ shortest-distance edges (mean degree 10). For every missing edge (u,v), Euclidean connection length c_{uv} and baseline shortest path length $d_G(u,v)$ were calculated. Their ratio defined the detour score in Equation (15).

$$\Delta_{uv} = \frac{d_G(u,v)}{c_{uv}} \tag{15}$$

The detour score favours spatially short connections that bypass relatively long routes in the current graph.

The principal screening procedure retained the nearer half of missing edges by Euclidean length and selected the ten highest detour scores, using node indices to resolve ties. Two alternative ten-edge sets were formed from the shortest missing links and a seeded random sample from the nearer half. Each screening rule defined a finite candidate set for exhaustive enumeration.

At most three links could be added, giving

$$\binom{10}{0} + \binom{10}{1} + \binom{10}{2} + \binom{10}{3} = 176 \tag{16}$$

With a maximum of three additions from ten candidate edges, each graph yielded $1 + 10 + 45 + 120 = 176$ feasible configurations, including the baseline. The principal detour-screened experiment therefore evaluated 2112 designs across 12 graphs. The alternative screening and attack ranking analyses were calculated separately.

Normalised spatial connection cost was calculated from the added Euclidean link length relative to the original graph's total edge length:

$$C_N(x) = \frac{\sum_{e \in E_c} \ell_e x_e}{\sum_{e \in E_0} \ell_e} \tag{17}$$

Here, E_c denotes the retained ten-edge candidate set, E_0 the original edge set, ℓ_e the Euclidean length of edge e, and $x_e \in \{0,1\}$ the edge selection variable. The denominator is fixed across the designs of a given graph. For each augmented graph $G + x$, degree-targeted deletion was ranked afresh at $q = 0$ and then held fixed along that graph's removal trajectory. The resilience index was normalised to the augmented graph's own initial efficiency. A parallel analysis applied the original baseline degree ranking to all augmented designs.

The Pareto illustration was selected using the spatial graph with the lower of the two central baseline resilience values among the 12 graphs (X_SFE_50_250_006). The reported best attainable values and nondominated sets refer to the enumerated candidate pool.

2.4. Worked Environmental Network Case

Graph models are widely used in ecology to examine connectivity and structural vulnerability [41–44], including food web responses to species loss [45–47]. The worked case uses the Catlins stream food web matrix from Thompson and Townsend [48], accessed through the Interaction Web Database [49]. The dataset contains 49 taxa and 110 directed trophic interactions. The matrix was symmetrised to obtain an undirected interaction network suitable for the study's connectivity and shortest path measures. This projection captures structural association among taxa while abstracting from trophic direction and ecological dynamics.

The Catlins disturbance curves summarise 500 random removal orders and the two fixed-baseline targeted-removal rules. Recovery curves follow deletion of the 30% highest-degree taxa. The archived trajectory series were integrated and checked against the corresponding resilience indices.

2.5. Computational Implementation and Statistical Analysis

Graph generation, simulation, and analysis were implemented in Python 3.13.5 with NetworkX 3.6.1 [50], NumPy 2.3.5 [51], SciPy 1.17.0, and pandas 2.2.3. A master random seed of 20261021 and phase-specific stream offsets of 100, 200, and 300 were used for disturbance, recovery, and redesign. Additional implementation details are provided in Supplementary Method S1.

Ninety-five percent confidence intervals were obtained from 1000 percentile-bootstrap resamples of independent graph instances. For paired contrasts, graph-level differences were resampled together to preserve matching. The descriptive standardised paired effect size d_z is defined in Equation (18).

$$d_z = \overline{\Delta}/s_\Delta \tag{18}$$

In Equation (18), Δ is the difference between two conditions on the same graph, $\overline{\Delta}$ is the mean paired difference across independent graph instances, and s_Δ is the sample standard deviation of these differences.

Analyses emphasised mean resilience, paired graph-level contrasts, confidence intervals, network size strata, restoration thresholds, and sensitivity to modelling choices. Spearman rank correlation assessed the association between efficiency-based resilience and the largest component measure. The independent graph instance was the bootstrap unit for synthetic network comparisons.

The disturbance analysis included 30 graphs for each topology–size combination ($n = 50, 100, 200$). Recovery contrasts used ten independent graphs per topology at $n = 100$, with 50 random order trajectories averaged within each graph. The spatial redesign analyses paired candidate selection and attack ranking conditions on 12 baseline graphs.

3. Results

3.1. Disturbance Resilience Across Graph Families

Figure 2 summarizes the main disturbance experiment.

Mean resilience under random removal varied from 0.5542 for SFE networks to 0.5601 for BA networks. Under degree- and betweenness-targeted deletion, BA resilience fell to 0.3776 and 0.3733, respectively, compared with 0.5116 and 0.5057 for ER networks. These patterns accord with established results on the targeted vulnerability of heterogeneous networks.

The mean random-minus-degree contrast was 0.1826 in BA networks and 0.0507 in ER networks (Table 1). The difference provides a useful paired task: apply the same threat scenarios to ER and BA graphs, then explain the influence of degree heterogeneity on the resulting resilience curves. Degree-targeted resilience in BA networks decreased from 0.4106 at $n = 50$ to 0.3807 at $n = 100$ and 0.3415 at $n = 200$, as illustrated in Supplementary Figure S1. The complete size-stratified results for random, degree-targeted, and betweenness-targeted removal are provided in Supplementary Table S1.

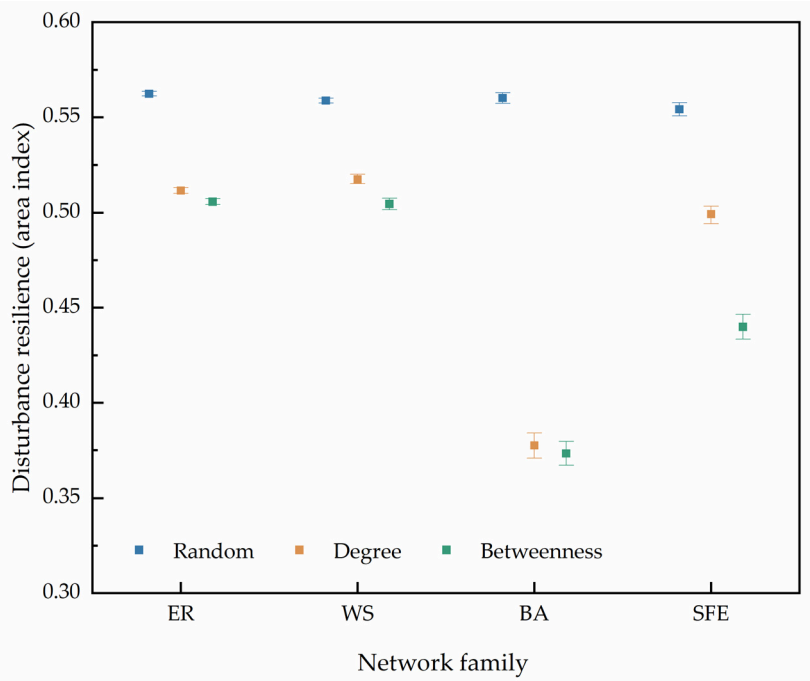


Figure 2. Mean efficiency-based disturbance resilience for ER, WS, BA, and SFE networks under random, degree-targeted, and betweenness-targeted removal (0–50% vertex loss). Error bars show 95% graph-level bootstrap confidence intervals.

Table 1. Paired within-graph disturbance resilience contrasts, averaged over 90 networks per family; intervals are 95% graph-level bootstrap confidence intervals.

Family	Contrast	Mean Difference	95% CI	d_z
ER	random—degree	0.0507	[0.0490, 0.0526]	5.8613
ER	random—betweenness	0.0566	[0.0545, 0.0584]	6.2262
WS	random—degree	0.0412	[0.0385, 0.0437]	3.2849
WS	random—betweenness	0.0542	[0.0511, 0.0571]	3.8670
BA	random—degree	0.1826	[0.1753, 0.1897]	5.3323
BA	random—betweenness	0.1868	[0.1806, 0.1932]	5.8973
SFE	random—degree	0.0550	[0.0483, 0.0617]	1.8166
SFE	random—betweenness	0.1143	[0.1076, 0.1214]	3.4077

3.2. Recovery Trajectories

Figure 3 summarizes the recovery experiment.

Restoration priorities showed a topology-dependent effect. In BA networks, mean recovery resilience was 0.6307 under random restoration, 0.6811 under degree priority, 0.6817 under betweenness priority, and 0.6786 under static initial efficiency gain priority. Early restoration of highly connected or bridging vertices can reconnect substantial parts of a heterogeneous network and improve performance during intermediate stages.

In ER networks, betweenness priority yielded 0.6951 versus 0.6848 under random restoration, a narrower contrast than in BA networks. WS and SFE trajectories further reflect clustering and spatial bottlenecks. In BA networks, mean T_{80} was 0.7533 under random restoration and 0.7000 under betweenness priority; the corresponding T_{90} values were 0.9000 and 0.8667. Supplementary Table S2 reports thresholds for all families and strategies.

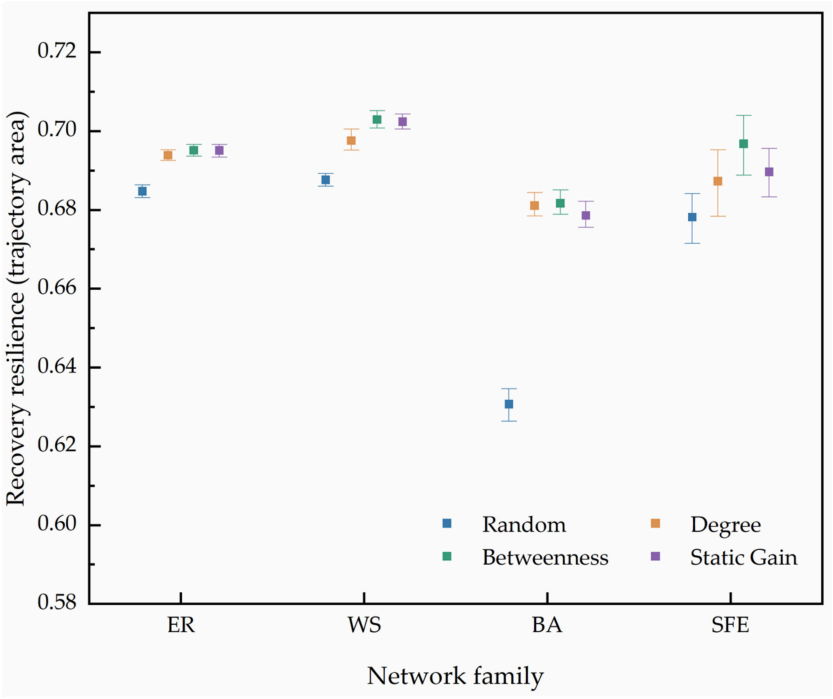


Figure 3. Mean recovery resilience trajectory areas for four restoration priorities across network families. Error bars indicate 95% graph-level bootstrap confidence intervals; the random-priority reference averages 50 orders per graph.

3.3. Constrained Redesign

The Redesign experiment enumerated 2112 feasible configurations across 12 spatial graphs with $n = 50$ and $m = 250$.

Figure 4 presents the mean best attainable degree-targeted disturbance resilience for zero to three additional links, selected from each graph's ten-edge detour pool.

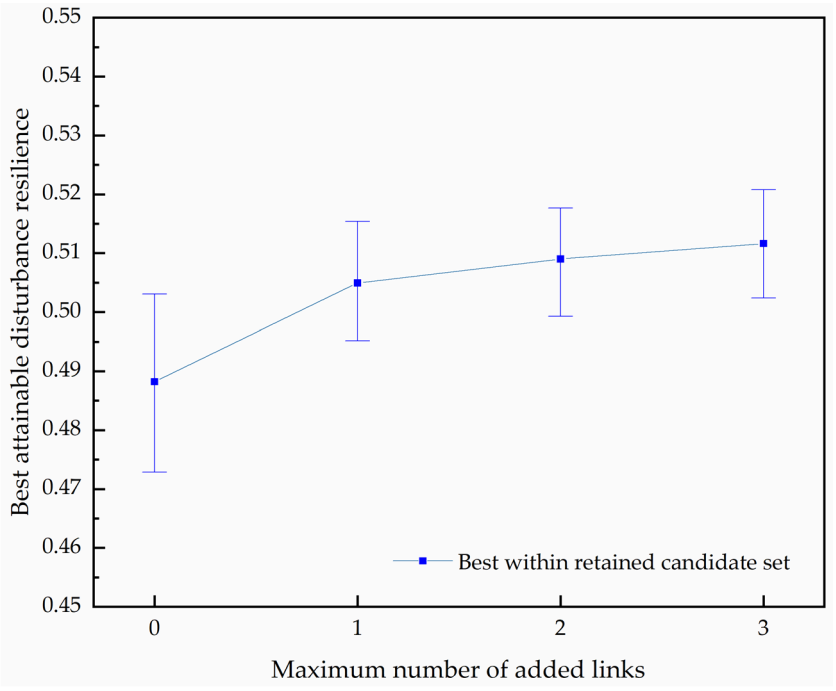


Figure 4. Mean best attainable degree-targeted disturbance resilience across 12 spatial graphs, for a maximum of zero to three added links from each graph's ten-edge detour set. Error bars denote 95% graph-level bootstrap confidence intervals.

Mean best attainable resilience rose from 0.4882 at the baseline to 0.5049 with one permitted link, 0.5090 with two, and 0.5116 with three. The separately generated redesign ensemble contained 50 vertices and 250 baseline edges per graph.

Marginal improvements decreased substantially with each additional link (Table 2). Average marginal improvements were 0.0167 for the first permitted link, 0.0041 for the second, and 0.0026 for the third.

Table 2. Marginal improvement in best attainable resilience as the permitted number of detour-screened links increases (12 spatial graphs; 95% bootstrap intervals).

Transition	Mean Marginal Gain	95% CI
0 to 1 links	0.0167	[0.0093, 0.0260]
1 to 2 links	0.0041	[0.0024, 0.0062]
2 to 3 links	0.0026	[0.0017, 0.0035]

Among 2100 non-empty configurations across the 12 graphs, 407 had a lower normalised resilience index than their corresponding baseline. Thus, link additions affected the relative performance measure differently across candidate designs.

Figure 5 shows eight nondominated resilience–cost designs for the selected spatial graph. Across all 12 graphs, 103 nondominated designs were identified (mean 8.58 per graph); graph-level baseline resilience, best attainable resilience, nondominated counts, and below-baseline link additions are reported in Supplementary Table S4. For up to three additions, the mean best attainable resilience was 0.5116 under detour screening, 0.4986 under shortest-link screening, and 0.5028 under random-nearby screening. The results illustrate the influence of candidate selection on the attainable resilience–cost options.

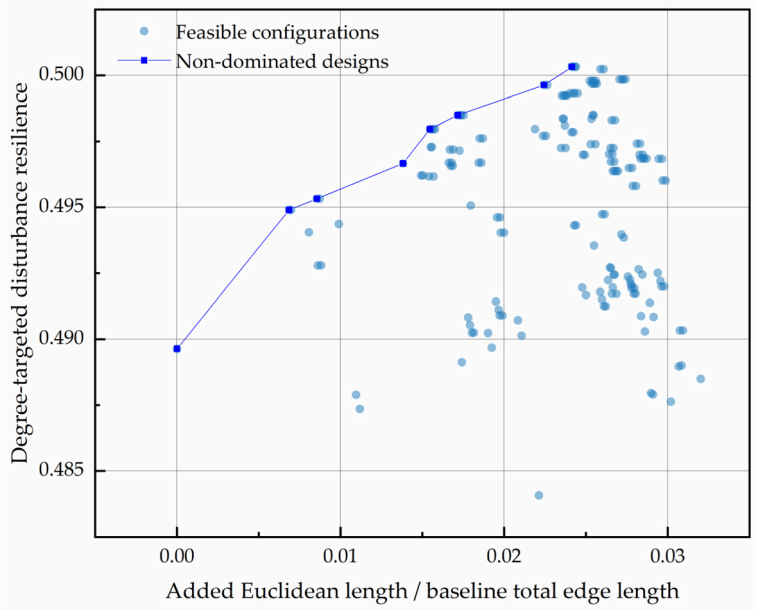


Figure 5. Resilience–cost Pareto frontier for spatial network X_SFE_50_250_006, selected as the lower-median baseline resilience case among the 12 spatial graphs. All 176 enumerated configurations are shown; the line connects nondominated designs within the ten-edge detour pool.

3.4. Robustness and Sensitivity Analyses

Sensitivity analyses covered the choice of resilience measure, network size, the number of retained detour candidates, and the candidate selection and attack ranking rules. Size-stratified results are provided in Supplementary Table S1, and redesign rule comparisons in Supplementary Table S3 and Figure S2.

Across 1080 graph disturbance observations, the efficiency-based and largest component resilience indices had a Spearman rank correlation of $\rho = 0.7226$. Through the removal rule, the association was 0.7558 for degree targeting, 0.7734 for betweenness targeting, and 0.2819 for random deletion. Targeted removals commonly reduce the size of the largest component while disrupting central shortest paths; random failures can change path lengths while retaining a substantial connected core. The two measures therefore offer complementary views of structural performance.

Detour-screened candidate sets of five, eight, and ten edges were compared on the same baseline graphs (Table 3). The analysis also contrasted the full ten-edge detour pool with shortest-link and random-nearby pools and compared attack rankings recomputed on $G + x$ with rankings fixed from the original graph.

Table 3. Mean best attainable resilience for nested detour candidate pools of 5, 8, and 10 edges across 12 spatial graphs; each column gives the maximum permitted number of added links.

Candidate Pool	1 Link	2 Links	3 Links	3-Link Gain
5	0.5046	0.5080	0.5092	4.46%
8	0.5049	0.5089	0.5105	4.73%
10	0.5049	0.5090	0.5116	4.96%

Note: The 3-link gain is the mean of graph-specific percentage gains relative to each baseline resilience, not the percentage change from group means.

With five detour candidates, the mean best attainable resilience reached 0.5092 for three permitted links, compared with 0.5116 for ten candidates. The largest average increment occurred at the first added link in each pool. In the separate attack-order comparison, the mean three-link optimum was 0.5116 when degree rankings were recomputed on $G + x$ and 0.5124 when the original baseline ranking was held fixed.

3.5. Worked Environmental Network Case: Catlins Stream Food Web

The symmetrised Catlins trophic interaction graph contained 49 taxa and 110 undirected interaction edges. Its density was 0.0935, mean degree 4.49, and average clustering coefficient 0.0308. The largest connected component contained 48 of 49 taxa.

Figure 6 presents disturbance trajectories for the undirected Catlins food web under random and targeted removal. Figure 7 illustrates recovery trajectories under alternative restoration strategies after removing the 30% highest-degree taxa.

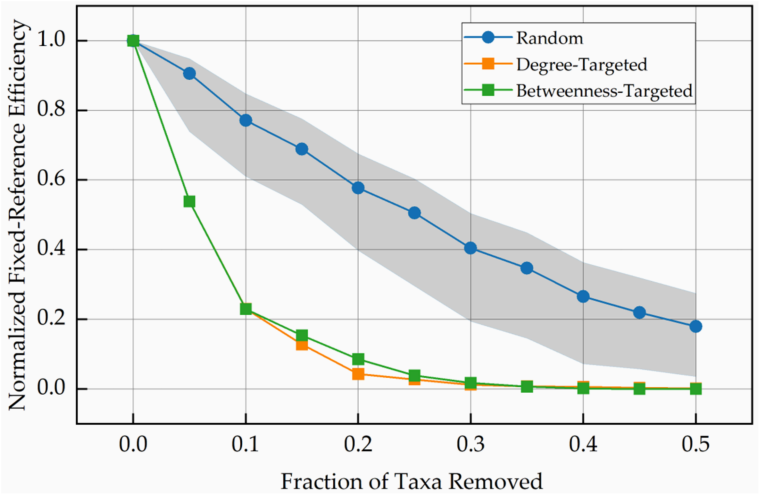


Figure 6. Disturbance trajectories for the undirected Catlins interaction graph under random and targeted removal. The shaded band denotes the 2.5th–97.5th percentile envelope across 500 random orders.

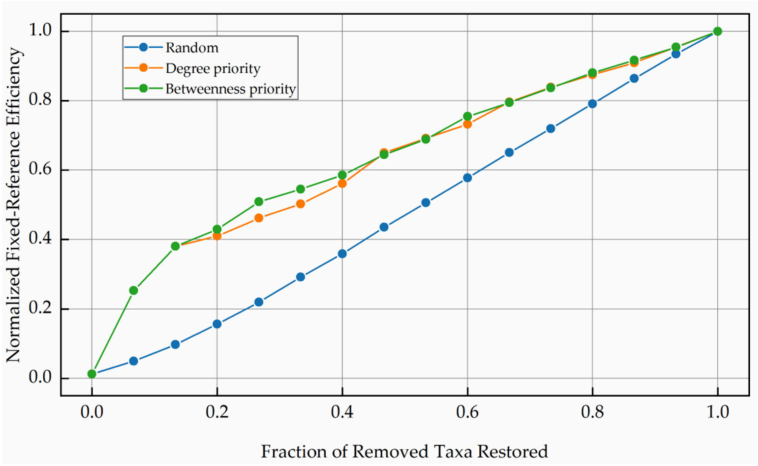


Figure 7. Recovery trajectories of the undirected Catlins interaction graph after removal of the 30% highest-degree taxa. Curves show fixed-reference efficiency during the restoration sequence.

Numerical integration of the Catlins disturbance trajectories yielded resilience indices of 0.5274, 0.1497, and 0.1572 under random, degree-targeted, and betweenness-targeted removal, respectively. Recovery-area indices were 0.4772 under random restoration, 0.6347 under degree priority, and 0.6452 under betweenness priority. The corresponding random restoration thresholds were $T_{80} = 0.8667$ and $T_{90} = 0.9333$; both structure-informed priorities reached $T_{80} = 0.7333$ and $T_{90} = 0.8667$. These indices characterise connectivity and efficiency in the undirected interaction network.

4. Discussion

4.1. Interpretation of the Computational Findings

Network vulnerability varied with graph topology and the disturbance mechanism. BA networks exhibited comparatively high resilience under random deletion and pronounced losses under targeted removal, reflecting the concentration of connectivity in high-degree vertices. The contrast between BA and ER networks supplies a mathematical comparison for the Remove phase: students can relate different resilience profiles to centrality distributions and attack rules.

Recovery adds the ordering of interventions to the analysis. In heterogeneous BA graphs, restoring central vertices early increases connectivity and short path accessibility during intermediate stages, while the more diffuse structure of ER graphs generally produces smaller priority effects. These patterns suggest tasks in which students compare restoration algorithms using trajectory areas, T_{80}/T_{90} thresholds, and the sequence of network states.

Redesign extends the sequence to network adaptation through proposed edge additions. A cardinality limit and spatial connection cost define a finite set of feasible interventions. The results show variation in relative disturbance resilience across candidate designs and screening rules, encouraging learners to examine topology, performance metrics, and intervention choices together.

Diminishing best-attainable marginal improvements and the Pareto frontiers offer a resource allocation task: students identify feasible alternatives, compare resilience and spatial cost, and justify a design under a specified disturbance scenario. The cost proxy and candidate edge screening rules make the decision assumptions available for inspection and sensitivity analysis.

4.2. Curricular and Methodological Contributions of R4-Graph

R4-Graph contributes a structured curricular connection among graph representation, disturbance analysis, restoration algorithms, and constrained design. A common graph provides continuity across four increasingly decision-oriented mathematical tasks. Each phase develops a distinct form of reasoning and produces a concrete artefact: a justified representation, a vulnerability profile, a restoration comparison, and a supported intervention choice.

The design draws on research on mathematical task design [52] and the planning of learning progressions through anticipated student reasoning [53]. Represent introduces choices of mathematical abstraction; Remove connects network structure to scenario-dependent outcomes; Recover develops algorithmic comparison over intermediate states; and Redesign asks students to formulate and defend resource-constrained choices. The five criteria in Section 2.1 and the sequence in Table 4 make this progression explicit.

Table 4. Four-stage task sequence for undergraduate discrete mathematics, showing mathematical objectives, proposed activities, and expected student work.

Phase	Mathematical Task and Learning Objective	Expected Student Artefact and Assessment Evidence
Represent	Define vertices, edges, spatial attributes, and modelling boundaries; justify the graph representation and compare alternative assumptions.	Labelled graph and adjacency matrix; explanation of edge semantics, assumptions, and a consequential modelling choice.
Remove	Compare random, degree-targeted, and betweenness-targeted removal; interpret efficiency and component trajectories in relation to network topology.	Labelled resilience curves and a written comparison of structural vulnerability under specified threats.
Recover	Compare restoration orders after a shared damaged state; compute trajectory areas and T80/T90 to assess the importance of restoration order.	Restoration rule or pseudocode, recovery curves, threshold values, and justification of a restoration priority.
Redesign	Evaluate screened candidate links under a cardinality constraint; compare spatial cost and targeted-removal resilience across feasible designs.	Resilience–cost comparisons, nondominated options, and a justified feasible network redesign.

The computational findings inform concrete design decisions. Contrasting BA and ER disturbance profiles supports a comparison task on topology and threat definition. Restoration trajectories and thresholds support tasks on ordering and cumulative performance. Sensitivity of augmented networks to candidate screening and attack ranking creates opportunities to revisit modelling choices. The cost–resilience frontier supports argumentation about feasible alternatives and competing objectives.

The Catlins case adds an authentic environmental graph for interpreting abstraction, connectivity, and disturbance. Its directed trophic information is projected into an undirected network, highlighting the importance of documenting representation choices. Spatial cost in Redesign likewise provides an interpretable resource proxy for examining constrained decisions.

4.3. Implications for Task and Curriculum Design

The intended setting is an upper-level undergraduate discrete mathematics or network modelling course for mathematics, engineering, or computer science students. Prerequisites include graph representations, adjacency matrices, connected components, shortest paths, basic algorithms, and elementary interpretation of quantitative plots. The proposed format is four 90 min sessions followed by a short individual report. Students may run Python

routines themselves or work with instructor-supplied networks and trajectories, depending on programming preparation.

All four sessions use a common spatial graph. In Represent, students construct a labelled graph and justify assumptions. In Remove, they compare random and centrality-targeted deletion using performance curves. In Recover, they implement or analyse restoration priorities and compare trajectory areas and thresholds. In Redesign, they evaluate candidate additions, identify nondominated resilience–cost options, and justify a feasible intervention under an explicit threat scenario.

Formative assessment can use four criteria: accuracy of the mathematical model, transparency of calculations, explanation of interactions between topology and operations, and justification of the chosen design. Each criterion is scored 0 (insufficient), 1 (partly supported), or 2 (well supported), giving a possible total of eight points. Table 4 links the tasks to student-produced evidence of these objectives.

For settings with limited programming time, the instructor can provide adjacency matrices, network files, or precomputed trajectories while retaining the explanation and decision components of each task. Students with programming experience can produce the full computational artefacts.

The artefacts form a cumulative learning sequence: the baseline graph and its assumptions support the Remove comparisons, recovery priorities refer to a damaged state of that model, and Redesign returns to its initial structure to evaluate new connections. This progression links graph computation to explanation and evidence-based choice.

4.4. Limitations and Future Directions

The study provides a computational analysis and an accompanying curriculum design. The proposed four-stage tasks and formative assessment criteria call for classroom evaluation through student work, instructor adaptations, and observed mathematical reasoning. This provides a basis for examining learning outcomes in subsequent studies.

The synthetic results depend on the selected graph generators, network sizes, fixed or recomputed removal rankings, and performance measures. The simulations used saved network instances, defined random seeds, and versioned software. The sensitivity analyses indicate the relevance of network size, candidate screening, and attack ranking to the reported comparisons.

The spatial experiment uses Euclidean length as a cost proxy and evaluates candidate additions screened by specified heuristics. Extending the analysis to actual infrastructure or ecological restoration would require context-specific cost data and additional network mechanisms. Further methodological comparisons could include larger candidate sets and global search benchmarks.

The next stage of educational research is to implement the tasks in undergraduate courses, document students' model choices and explanations, and analyse how they compare recovery algorithms and justify constrained designs. Iterative trials can refine the task sequence, time allocations, and assessment rubric while evaluating sustainability-oriented reasoning [54].

5. Conclusions

R4-Graph organises sustainability-oriented graph theory through a four-stage sequence of representation, disturbance analysis, recovery, and redesign. Its contribution is a connected set of mathematically specified tasks that advances from network modelling to algorithms and resource-constrained decisions on a common graph.

The computational experiments documented topology-dependent disturbance resilience, changes in recovery trajectories under alternative priorities, and resilience–cost

trade-offs in spatial redesign. Network size comparisons, recovery thresholds, performance-measure sensitivity, and alternative edge screens further characterised these results. The Catlins stream food web illustrated how the same graph-theoretic measures can be applied to an environmental interaction network.

The proposed teaching sequence connects these numerical contrasts to undergraduate learning objectives, student-produced mathematical artefacts, and an explicit framework for interpreting and justifying network decisions. Classroom implementation and evaluation provide the next stage of development.

Supplementary Materials: The following supporting information can be downloaded at https://www.mdpi.com/article/10.3390/su182111240/s1, Supplementary Method S1: Computational protocol; Figure S1: Network size effects on degree-targeted disturbance resilience; Figure S2: Sensitivity to candidate edge screening and attack ranking rules; Table S1: Disturbance resilience across network sizes and removal mechanisms; Table S2: Recovery resilience and threshold measures; Table S3: Comparison of candidate edge screening methods; Table S4: Pareto frontier characteristics across 12 spatial networks.

Author Contributions: Conceptualization, R.Z. and Y.Y.; methodology, Y.Y. and L.L.; formal analysis, L.L. and C.L.; writing—original draft preparation, R.Z. and C.L.; writing—review and editing, Y.Y. and L.L.; supervision, Y.Y. All authors have read and agreed to the published version of the manuscript.

Funding: This research was partly supported by the Educational and Teaching Reform Research and Practice Project of North China University of Science and Technology (L2450); the Virtual Learning and Research Office Project for College Mathematics Courses Group of the Ministry of Education of China (North China University of Science and Technology), Hebei Province Graduate Course Ideological and Political Demonstration Course Project (YKCSZ2024063).

Institutional Review Board Statement: Not applicable.

Informed Consent Statement: Not applicable.

Data Availability Statement: The Catlins stream food web interaction data are publicly accessible through the Interaction Web Database (IWDB) [49], with the original study acknowledged in [48]. The computational results supporting this study are presented in the manuscript and Supplementary Materials. The complete computational archive for the revised experiments, including Python source code, environment specifications, random seeds, generated synthetic graphs, graph-level results, sensitivity analyses, figure scripts, and the available archived Catlins trajectory data, is available from the corresponding author upon reasonable request. The original Catlins food web interaction matrix is not redistributed.

Acknowledgments: During the preparation of this manuscript, the authors used ChatGPT (OpenAI, GPT-6) for English-language polishing and grammar checking. The authors have reviewed and edited the output and take full responsibility for the content of this publication.

Conflicts of Interest: The authors declare no conflicts of interest.

References

1. Sandefur, J.; Lockwood, E.; Hart, E.; Greefrath, G. Teaching and learning discrete mathematics. *ZDM Math. Educ.* **2022**, *54*, 753–775. [CrossRef]
2. Greefrath, G.; Siller, H.-S.; Vorhölter, K.; Kaiser, G. Mathematical modelling and discrete mathematics: Opportunities for modern mathematics teaching. *ZDM Math. Educ.* **2022**, *54*, 865–879. [CrossRef] [PubMed]
3. Hart, E.W.; Martin, W.G. Discrete mathematics is essential mathematics in a 21st century school curriculum. In *Teaching and Learning Discrete Mathematics Worldwide: Curriculum and Research*; Hart, E.W., Sandefur, J., Eds.; Springer: Cham, Switzerland, 2018; pp. 3–19.
4. UNESCO. *Education for Sustainable Development Goals: Learning Objectives*; UNESCO: Paris, France, 2017.
5. UNESCO. *Education for Sustainable Development: A Roadmap*; UNESCO: Paris, France, 2020.
6. Wiek, A.; Withycombe, L.; Redman, C.L. Key competencies in sustainability: A reference framework for academic program development. *Sustain. Sci.* **2011**, *6*, 203–218. [CrossRef]

7. Brundiers, K.; Barth, M.; Cebrián, G.; Cohen, M.; Diaz, L.; Doucette-Remington, S.; Dripps, W.; Habron, G.; Harré, N.; Jarchow, M.; et al. Key competencies in sustainability in higher education—Toward an agreed-upon reference framework. *Sustain. Sci.* **2021**, *16*, 13–29. [CrossRef]
8. Rieckmann, M. Future-oriented higher education: Which key competencies should be fostered through university teaching and learning? *Futures* **2012**, *44*, 127–135. [CrossRef]
9. Barth, M.; Godemann, J.; Rieckmann, M.; Stoltenberg, U. Developing key competencies for sustainable development in higher education. *Int. J. Sustain. High. Educ.* **2007**, *8*, 416–430. [CrossRef]
10. Lozano, R.; Merrill, M.Y.; Sammalisto, K.; Ceulemans, K.; Lozano, F.J. Connecting competences and pedagogical approaches for sustainable development in higher education: A literature review and framework proposal. *Sustainability* **2017**, *9*, 1889. [CrossRef]
11. Suh, H.; Han, S. Promoting sustainability in university classrooms using a STEM project with mathematical modeling. *Sustainability* **2019**, *11*, 3080. [CrossRef]
12. Suh, H.; Kim, S.; Hwang, S.; Han, S. Enhancing preservice teachers' key competencies for promoting sustainability in a university statistics course. *Sustainability* **2020**, *12*, 9051. [CrossRef]
13. Green, C.; Molloy, O.; Duggan, J. An empirical study of the impact of systems thinking and simulation on sustainability education. *Sustainability* **2022**, *14*, 394. [CrossRef]
14. Su, C.S.; Díaz-Levicoy, D.; Vásquez, C.; Hsu, C.C. Sustainable development education for training and service teachers teaching mathematics: A systematic review. *Sustainability* **2023**, *15*, 8435. [CrossRef]
15. Makramalla, M.; Coles, A.; le Roux, K.; Wagner, D. Mathematics education for sustainable futures: A strengths-based survey of the field to invite further research action. *Educ. Stud. Math.* **2025**, *119*, 535–556. [CrossRef]
16. Just, J.; Siller, H.-S.; Vorhölter, K. Directions of intentionalities in education for sustainable development in mathematics education: A systematic literature review. *Educ. Stud. Math.* **2026**, *121*, 499–523. [CrossRef]
17. Hauge, K.H.; Barwell, R. Post-normal science and mathematics education in uncertain times: Educating future citizens for extended peer communities. *Futures* **2017**, *91*, 25–34. [CrossRef]
18. Weber, J.M.; Lindenmeyer, C.P.; Lio, P.; Lapkin, A.A. Teaching sustainability as complex systems approach: A sustainable development goals workshop. *Int. J. Sustain. High. Educ.* **2021**, *22*, 25–41. [CrossRef]
19. Holling, C.S. Resilience and stability of ecological systems. *Annu. Rev. Ecol. Syst.* **1973**, *4*, 1–23. [CrossRef]
20. Bruneau, M.; Chang, S.E.; Eguchi, R.T.; Lee, G.C.; O'Rourke, T.D.; Reinhorn, A.M.; Shinozuka, M.; Tierney, K.; Wallace, W.A.; von Winterfeldt, D. A framework to quantitatively assess and enhance the seismic resilience of communities. *Earthq. Spectra* **2003**, *19*, 733–752. [CrossRef]
21. Hosseini, S.; Barker, K.; Ramirez-Marquez, J.E. A review of definitions and measures of system resilience. *Reliab. Eng. Syst. Saf.* **2016**, *145*, 47–61. [CrossRef]
22. Francis, R.; Bekera, B. A metric and frameworks for resilience analysis of engineered and infrastructure systems. *Reliab. Eng. Syst. Saf.* **2014**, *121*, 90–103. [CrossRef]
23. Linkov, I.; Bridges, T.; Creutzig, F.; Decker, J.; Fox-Lent, C.; Kröger, W.; Lambert, J.H.; Levermann, A.; Montreuil, B.; Nathwani, J.; et al. Changing the resilience paradigm. *Nat. Clim. Change* **2014**, *4*, 407–409. [CrossRef]
24. Ouyang, M. Review on modeling and simulation of interdependent critical infrastructure systems. *Reliab. Eng. Syst. Saf.* **2014**, *121*, 43–60. [CrossRef]
25. Poulin, C.; Kane, M.B. Infrastructure resilience curves: Performance measures and summary metrics. *Reliab. Eng. Syst. Saf.* **2021**, *216*, 107926. [CrossRef]
26. Newman, M.E.J. *Networks: An Introduction*; Oxford University Press: Oxford, UK, 2010.
27. Boccaletti, S.; Latora, V.; Moreno, Y.; Chavez, M.; Hwang, D.-U. Complex networks: Structure and dynamics. *Phys. Rep.* **2006**, *424*, 175–308. [CrossRef]
28. Barrat, A.; Barthélemy, M.; Pastor-Satorras, R.; Vespignani, A. The architecture of complex weighted networks. *Proc. Natl. Acad. Sci. USA* **2004**, *101*, 3747–3752. [CrossRef] [PubMed]
29. Holme, P.; Kim, B.J.; Yoon, C.N.; Han, S.K. Attack vulnerability of complex networks. *Phys. Rev. E* **2002**, *65*, 056109. [CrossRef] [PubMed]
30. Cohen, R.; Erez, K.; ben-Avraham, D.; Havlin, S. Resilience of the Internet to random breakdowns. *Phys. Rev. Lett.* **2000**, *85*, 4626–4628. [CrossRef] [PubMed]
31. Callaway, D.S.; Newman, M.E.J.; Strogatz, S.H.; Watts, D.J. Network robustness and fragility: Percolation on random graphs. *Phys. Rev. Lett.* **2000**, *85*, 5468–5471. [CrossRef] [PubMed]
32. Schneider, C.M.; Moreira, A.A.; Andrade, J.S., Jr.; Havlin, S.; Herrmann, H.J. Mitigation of malicious attacks on networks. *Proc. Natl. Acad. Sci. USA* **2011**, *108*, 3838–3841. [CrossRef] [PubMed]
33. Ehrgott, M. *Multicriteria Optimization*, 2nd ed.; Springer: Berlin/Heidelberg, Germany, 2005.
34. Latora, V.; Marchiori, M. Efficient behavior of small-world networks. *Phys. Rev. Lett.* **2001**, *87*, 198701. [CrossRef] [PubMed]
35. Freeman, L.C. A set of measures of centrality based on betweenness. *Sociometry* **1977**, *40*, 35–41. [CrossRef]

36. Freeman, L.C. Centrality in social networks: Conceptual clarification. *Soc. Netw.* **1978**, *1*, 215–239. [CrossRef]
37. Erdős, P.; Rényi, A. On random graphs I. *Publ. Math. Debr.* **1959**, *6*, 290–297.
38. Watts, D.J.; Strogatz, S.H. Collective dynamics of small-world networks. *Nature* **1998**, *393*, 440–442. [CrossRef] [PubMed]
39. Barabási, A.-L.; Albert, R. Emergence of scaling in random networks. *Science* **1999**, *286*, 509–512. [CrossRef] [PubMed]
40. Penrose, M. *Random Geometric Graphs*; Oxford University Press: Oxford, UK, 2003.
41. Urban, D.; Keitt, T. Landscape connectivity: A graph-theoretic perspective. *Ecology* **2001**, *82*, 1205–1218. [CrossRef]
42. Minor, E.S.; Urban, D.L. Graph theory as a proxy for spatially explicit population models in conservation planning. *Ecol. Appl.* **2007**, *17*, 1771–1782. [CrossRef] [PubMed]
43. Saura, S.; Pascual-Hortal, L. A new habitat availability index to integrate connectivity in landscape conservation planning: Comparison with existing indices and application to a case study. *Landsc. Urban Plan.* **2007**, *83*, 91–103. [CrossRef]
44. Rayfield, B.; Fortin, M.-J.; Fall, A. Connectivity for conservation: A framework to classify network measures. *Ecology* **2011**, *92*, 847–858. [CrossRef] [PubMed]
45. Solé, R.V.; Montoya, J.M. Complexity and fragility in ecological networks. *Proc. R. Soc. B* **2001**, *268*, 2039–2045. [CrossRef] [PubMed]
46. Dunne, J.A.; Williams, R.J.; Martinez, N.D. Network structure and biodiversity loss in food webs: Robustness increases with connectance. *Ecol. Lett.* **2002**, *5*, 558–567. [CrossRef]
47. Memmott, J.; Waser, N.M.; Price, M.V. Tolerance of pollination networks to species extinctions. *Proc. R. Soc. B* **2004**, *271*, 2605–2611. [CrossRef] [PubMed]
48. Thompson, R.M.; Townsend, C.R. Impacts on stream food webs of native and exotic forest: An intercontinental comparison. *Ecology* **2003**, *84*, 145–161. [CrossRef]
49. Interaction Web Database (IWDB). Thompson and Townsend (Multiple Sources): Catlins [Dataset]. Available online: https://www.ecologia.ib.usp.br/iwdb/html/thomps_towns.html (accessed on 22 October 2026).
50. Hagberg, A.A.; Schult, D.A.; Swart, P.J. Exploring network structure, dynamics, and function using NetworkX. In *Proceedings of the 7th Python in Science Conference (SciPy2008), Pasadena, CA, USA, 19–24 August 2008*; SciPy: Pasadena, CA, USA, 2008; pp. 11–15.
51. Harris, C.R.; Millman, K.J.; van der Walt, S.J.; Gommers, R.; Virtanen, P.; Cournapeau, D.; Wieser, E.; Taylor, J.; Berg, S.; Smith, N.J.; et al. Array programming with NumPy. *Nature* **2020**, *585*, 357–362. [CrossRef] [PubMed]
52. Watson, A.; Ohtani, M. (Eds.) *Task Design in Mathematics Education: An ICMI Study 22*; Springer: Cham, Switzerland, 2015.
53. Simon, M.A. Reconstructing mathematics pedagogy from a constructivist perspective. *J. Res. Math. Educ.* **1995**, *26*, 114–145. [CrossRef]
54. Prediger, S.; Gravemeijer, K.; Confrey, J. Design research with a focus on learning processes: An overview on achievements and challenges. *ZDM Math. Educ.* **2015**, *47*, 877–891. [CrossRef]

Disclaimer/Publisher's Note: The statements, opinions and data contained in all publications are solely those of the individual author(s) and contributor(s) and not of MDPI and/or the editor(s). MDPI and/or the editor(s) disclaim responsibility for any injury to people or property resulting from any ideas, methods, instructions or products referred to in the content.